


# Ground-state structure and physical properties of $YB_3$ predicted from first-principles calculations

Bin-Hua Chu(初斌华)†, Yuan Zhao(赵元), and De-Hua Wang(王德华)

**Citation:**Chin. Phys. B, 2021, 30 (**4**): 046101. DOI: 10.1088/1674-1056/abcf94
Journal homepage: http://cpb.iphy.ac.cn; http://iopscience.iop.org/cpb

**What follows is a list of articles you may be interested in**

---

## *Ab initio* study on crystal structure and phase stability of $ZrC_2$ under high pressure

Yong-Liang Guo(郭永亮), Jun-Hong Wei(韦俊红), Xiao Liu(刘潇), Xue-Zhi Ke(柯学志), and Zhao-Yong Jiao(焦照勇)

Chin. Phys. B, 2021, 30 (**1**): 016101. DOI: 10.1088/1674-1056/abb3e7

## Effects of Re, Ta, and W in [110] (001) dislocation core of $\gamma/\gamma'$ interface to Ni-based superalloys: First-principles study

Chuanxi Zhu(朱传喜), Tao Yu(于涛)

Chin. Phys. B, 2020, 29 (**9**): 096101. DOI: 10.1088/1674-1056/abad26

## Tunable electronic structures of germanane/antimonene van der Waals heterostructures using an external electric field and normal strain

Xing-Yi Tan(谭兴毅), Li-Li Liu(刘利利), Da-Hua Ren(任达华)

Chin. Phys. B, 2020, 29 (**7**): 076102. DOI: 10.1088/1674-1056/ab8a39

## Theoretical study on martensitic-type transformation path from rutile phase to $\alpha$-$PbO_2$ phase of $TiO_2$

Wen-Xuan Wang(王文轩), Zhen-Yi Jiang(姜振益), Yan-Ming Lin(林彦明), Ji-Ming Zheng(郑继明), Zhi-Yong Zhang(张志勇)

Chin. Phys. B, 2020, 29 (**7**): 076101. DOI: 10.1088/1674-1056/ab8abe

## First-principles calculations of solute-vacancy interactions in aluminum

Sha-Sha Zhang(张莎莎), Zheng-Jun Yao(姚正军), Xiang-Shan Kong(孔祥山), Liang Chen(陈良), Jing-Yu Qin(秦敬玉)

Chin. Phys. B, 2020, 29 (**6**): 066103. DOI: 10.1088/1674-1056/ab8458

---

# Ground-state structure and physical properties of $YB_3$ predicted from first-principles calculations*

Bin-Hua Chu(初斌华)†, Yuan Zhao(赵元), and De-Hua Wang(王德华)

*School of Physics and Opto-Electronic Engineering, Ludong University, Yantai* 264025, *China*

(Received 22 October 2020; revised manuscript received 16 November 2020; accepted manuscript online 2 December 2020)

Using the calypso algorithm with first-principles calculations, we have predicted two orthorhombic *Cmmm* and *Pmmm* structures for $YB_3$. The new structures are energetically much better than the previously proposed $WB_3$-type, $ReB_3$-type, $FeB_3$-type, and $TcP_3$-type structures. We find that the *Cmmm* phase transforms to the *Pmmm* phase at about 31 GPa. Subsequent calculations show that the *Cmmm* phase is mechanical and dynamical stable at ambient conditions. The analysis of the chemical bonding properties indicates that there are strong B–B bonds that make considerable contributions to its stability.

**Keywords:** first-principles, high pressures, convex hull

**PACS:** 61.50.Ah, 61.50.Ks, 61.66.Fn **DOI:** 10.1088/1674-1056/abcf94

## 1. Introduction

Superhard materials are widely used in industrial applications such as abrasive substance and polishing tools to wear-resistant coatings.[1–3] The most well-known superhard materials are diamond and *c*-BN. At present, the diamond is still the most rigid and the best thermal conducting material. However, over 800 °C, diamond reacts readily with ferrous metals.[4] The hardness of cubic boron nitride (*c*-BN) is between 32 GPa and 50 GPa.[5] Unfortunately, it has to be synthesized at high pressure and high-temperature condition, which needs tremendous cost. This makes them expensive and rare.[6–9] Recently, we find that intercalating light elements (boron, carbon, nitrogen, or oxygen) into transition metals could be the right way for searching for potential superhard materials. These compounds, with strong directional covalent bonds, can effectively increase the resistance against the plastic deformations in no small extent. As we all know, the crystal structure is the key to solving the mechanical properties of materials. Therefore, researchers strive to explore novel superhard materials. Recently, many transition metal compounds have been studied, such as $ReB_2$, $OsB_2$, $RuO_2$, $WN_2$, and $WB_4$.[10–17] In these borides, boron rich compounds, such as transition metal (TM) tetraborides and TM triborides have attracted a lot of attention. These compounds are expected to have high bulk and shear moduli. Moreover, they usually form the three-dimensional (3D) covalent bond networks, for example, $CrB_4$, $WB_4$, $FeB_4$, $MnB_4$, $VB_4$, $MoB_4$, and $HfB_4$.[18–31] According to the report, the hardness of $CrB_4$ is 48 GPa and the hardness of $WB_4$ is 43 GPa. These compounds are regarded as superhard materials. Unfortunately, subsequent studies revealed that the $WB_3$ and $MoB_3$ are more stable than the earlier mentioned $WB_4$ and $MoB_4$ structures, and they have unique mechanical properties.[32] An idea raises: Will TM triborides with these similar structures be stable? Whether they have better physical properties? In this situation, many TM triborides, such as $TaB_3$, $OsB_3$, $TcB_3$, $RuB_3$, $MoB_3$, $ReB_3$, $CrB_3$, $IrB_3$, $HfB_3$, and $ScB_3$ have been explored and discussed in many works.[33–42] In 2014, Zhang *et al.* predicted two orthorhombic *Cmcm* and *Amm*2 structures for $ZrB_4$. The two structures have large shear modulus and high hardness (42.8 GPa for *Cmcm* and 42.6 GPa for *Amm*2).[43] They are all potentially superhard materials. A few more years passed, Zhang *et al.* predicted a novel *C*2/*m* phase for $ZrB_3$. The hardness of this phase is up to 42 GPa. The strong covalent bonding contributes to the high hardness for $ZrB_3$.[44] Yttrium is adjacent to the zirconium in the periodic table, so we expect that boron-rich yttrium borides may have good physics properties. In previous studies, there are four phases can be experimentally observed ($YB_2$, $YB_4$, $YB_6$, and $YB_{12}$) in Y–B systems.[45,46] However, the ground state structure of $YB_3$ has never been solved theoretically or experimentally up to now. Therefore, exploring the crystal structure of $YB_3$ has an essential significance for high boron contents in Y–B systems.

In the present work, the particle swarm optimization (PSO) algorithm for crystal structure prediction is used to explore the crystal structures of $YB_3$. A novel *Cmmm* structure for $YB_3$ has been revealed under ambient conditions by using the CALYPSO crystal structure prediction method. This method has successfully confirmed by experiments. In our work, the *Cmmm*-$YB_3$ structure is energetically preferable to previously predicted $WB_3$-type, $ReB_3$-type, $FeB_3$-

*Project supported by the Young Scientists Fund of the National Natural Science Foundation of China (Grant Nos. 11704170 and 61705097) and the Natural Science Foundation of Shandong Province, China (Grant Nos. ZR2016AP02, ZR2016EMP01, and ZR2019MA066).

†Corresponding author. E-mail: chubinhua0125@126.com

© 2021 Chinese Physical Society and IOP Publishing Ltd 

type, and $TcP_3$-type structures. The stability of *Cmmm*-$YB_3$ is confirmed through the study of the elastic constants and phonon. Besides, we also explore the formation enthalpy, elastic constants, and bonding properties of *Cmmm*-$YB_3$ by first-principle calculations.

## 2. Computation details

In this work, the PSO methodology on crystal structural prediction has been performed in the CALYPSO. We have searched the potential crystal structures of $YB_3$ under ambient conditions containing 1–4 formula units in each simulation cell. CALYPSO has successfully solved the structures of various systems requiring only chemical compositions and specified external conditions.[47–49] The calculations are implemented in the Vienna *ab initio* simulation package (VASP) code.[50–52] The generalized gradient approximation (GGA) with the projector-augmented wave (PAW) potential is treated as the exchange–correlation functional.[53,54] The energy cutoff 500 eV and appropriate Monkhorst–Pack *k* meshes are chosen. Monkhorst–Pack *k* meshes of 3×4×8 for *Cmmm* phase, 8×3×10 for *Pmmm* phase, 7×7×5 for $WB_3$-type structure, 13×13×7 for $ReB_3$-type structure, 8×12×6 for $FeB_3$-type structure, and 2×11×6 for $TcP_3$-type structure. For hexagonal structures, we use $\Gamma$-centered grids. The formation enthalpy of $Y_mB_n$ is confirmed by the following equation: $\Delta H = H(Y_mB_n) - mH(Y) - nH(B)$, in here, the solid $\alpha$-$B_{12}$ element is considered as the referenced phases.[55] The phonon calculation is carried out in the PHONOPY code.[56,57] The calculated bulk modulus B and shear modulus *G* is obtained by the strain–stress method. The theoretical Vicker's hardness is estimated by Chen's model.[58]

## 3. Results and discussion

In the present work, a new orthorhombic *Cmmm* structure is revealed by the CALYPSO crystal structure prediction method. The orthorhombic *Cmmm* structure includes six $YB_3$ f.u. ($a = 11.598$ Å, $b = 7.761$ Å, $c = 3.491$ Å, $\alpha = \beta = \gamma = 90°$) in a unit cell at ambient conditions. The metal Y atoms have the Wyckoff 4i (0, 0.8093,0) and 4g (0.2754, 0, 0) sites, and the four B atoms are at the Wyckoff 8q (0.4214, 0.8829, 0.5), 8q (0.3247, 0.7144, 0.5), 4h (0.8806, 0, 0.5), and 4l (0, 0.5, 0.7959) sites, respectively. The polyhedral view for the predicted *Cmmm* structure is presented in Fig. 1. We can see that the *Cmmm* structure can be described as the alternative arrangement by Y atoms and puckered network formed by B atoms, there is an interesting B–Y–B sandwich stacking sequence along the *c* axis.

For further investigate the stabilities of different $YB_3$ phases, we calculated the total energy per formula unit vs volume for these two candidate structures. For comparison, the four possible structures of the known TM compounds: $WB_3$ ($P6_3/mmc$, No. 194), $ReB_3$ ($P\bar{6}m2$, No. 187), $FeB_3$ ($P2_1/m$, No. 11), and $TcP_3$ (*Pnma*, No. 62) are also considered as the potential phase for $YB_3$, and we define them as the $WB_3$-, $ReB_3$-, $FeB_3$-, and $TcP_3$-type structures. The *E*–*V* curves of all considered phases of $YB_3$ are illustrated in Fig. 2. Among these six considered structures, at first, the *Pmmm* phase has the lowest total energy minimum. However, with the increase of volume, we can see that the predicted *Cmmm* phase of $YB_3$ is lower in energy than the other phases. There is a phase transition process in our calculations. For aiding experimental synthesis in future, we explore the thermodynamic stability of $YB_3$. The predicted *Cmmm* structure concerning the separate phases is investigated by the reaction route $\Delta H = H(YB_3) - H(Y) - 3H(B)$. The Y (space group: *Fm*-3*m*) and $\alpha$-Boron (space group: *R*-3*m*) are chosen as the referenced phases. From Fig. 3, it can be seen that the *Cmmm* phase has the negative formation enthalpy at about −2.2 eV at ambient conditions, indicating that the *Cmmm* phase is thermodynamic stable and can be synthesized by elemental yttrium and boride. As the pressure increases, the stabilities of the *Cmmm* phase is gradually decreased. When the increasing pressure comes over 31 GPa, the phase transforms from the *Cmmm* phase to the *Pmmm* phase, indicating that the *Pmmm* phase is a high-pressure phase and more energetically stable at high pressure.

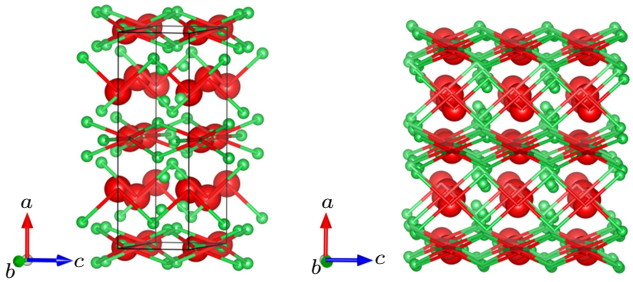



**Fig. 1.** Crystal structure of *Cmmm*-$YB_3$. Small green spheres represent boron atoms and large red spheres represent yttrium atoms, respectively.

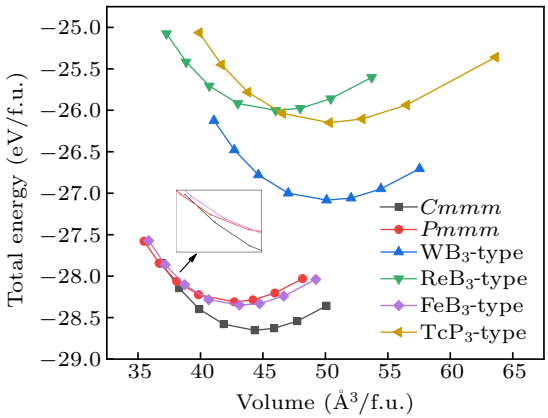



**Fig. 2.** The total energy per f.u. volume for $YB_3$ as a function of volume with six different structures.

Figure 4 presents the relative enthalpy-pressure curves of the *Cmmm*-$YB_3$ and *Pmmm*-$YB_3$ structures concerning the el-

emental Y and B under the pressure up to 100 GPa. Here we choose $YB_2$ (*P6/mmm*, No. 191), $YB_4$ (*P4/mbm*, No. 127), $YB_6$ (*Pm*$\bar{3}$*m*, No. 221), and $YB_{12}$ (*Fm*$\bar{3}$*m*, No. 225) as the competing phases in our calculations. From Fig. 4, we can see that the *Cmmm* phase is more stable than the compound $YB_{12}$+Y, $YB_6$+$YB_{12}$+Y, and $YB_2$+B in the whole pressure range, while the competing phase $YB_2$+$YB_4$ becomes the most stable phase underneath 86 GPa. As the pressure is greater than 86 GPa, the predicted *Pmmm* phase is energetically the most stable phase against to decompose into the compound $YB_2$+$YB_4$.

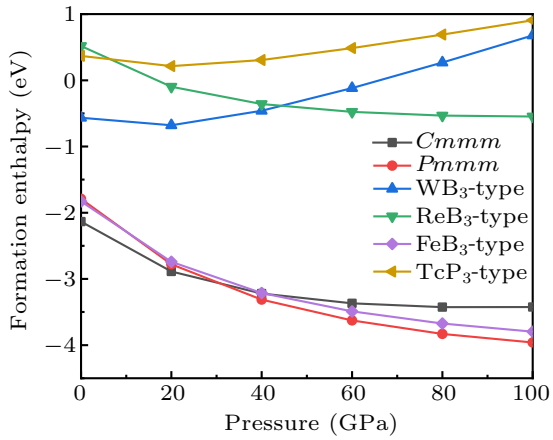



**Fig. 3.** Formation enthalpis *versus* pressure for different yttrium borides structures.

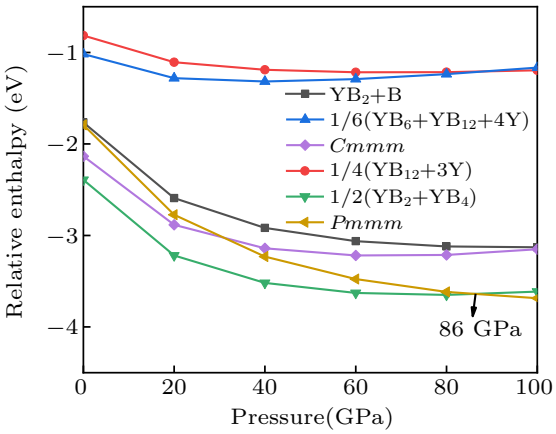



**Fig. 4.** The relative enthalpy–pressure diagrams of the *Cmmm*-$YB_3$, *Pmmm*-$YB_3$ and its respective competing phases with respect to elemental Y and B. The $\alpha$-B (0 GPa–19 GPa), $\gamma$-B (19 GPa–89 GPa), and $\alpha$-Ga phase (89 GPa–100 GPa) were used in the calculations.

To further verify the stability of the *Cmmm* and *Pmmm* structures, we present the convex hull plots. We know that all the structures lie on a convex hull could be seen as thermodynamically stable and composable in theory. From Fig. 4, the stability of the predicted *Pmmm* phase is superior to the competing phase $YB_2$+$YB_4$ above 86 GPa, so we calculate the convex hull under the pressure of 100 GPa. The convex hull plots of the Y–B system at the selected pressures are depicted in Fig. 5. From the convex hull in Fig. 5(a), all enthalpies of formation of these compounds are negative, and four stable stoichiometry ($YB_2$, $YB_4$, $YB_6$, and $YB_{12}$) appear in our convex hull plots. Our proposed *Cmmm*-$YB_3$ is located above the curve of the convex hull, suggesting it is unstable and is going to decompose. Furthermore, from Fig. 5(b), the *Pmmm* structure exactly sits on the curves of the convex hull, indicating it is stable and will not decompose.

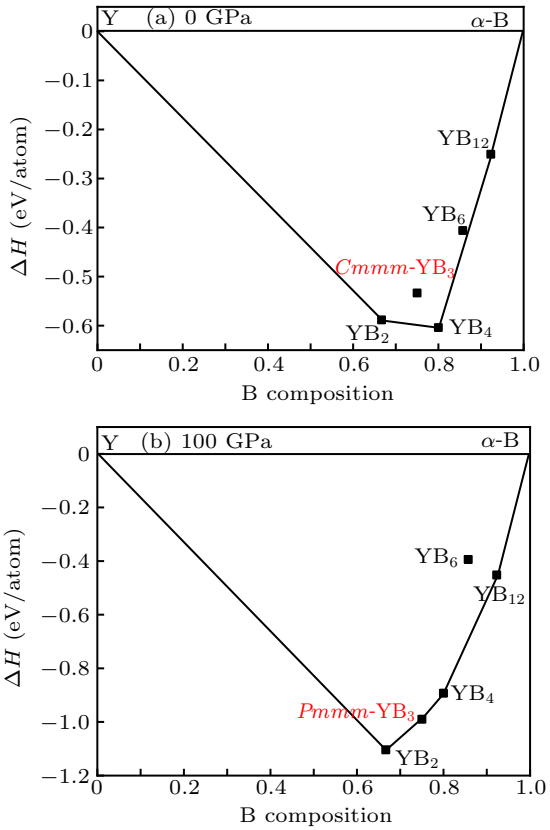



**Fig. 5.** The convex hulls of $YB_3$ at the pressure of (a) 0 GPa and (b) 100 GPa.

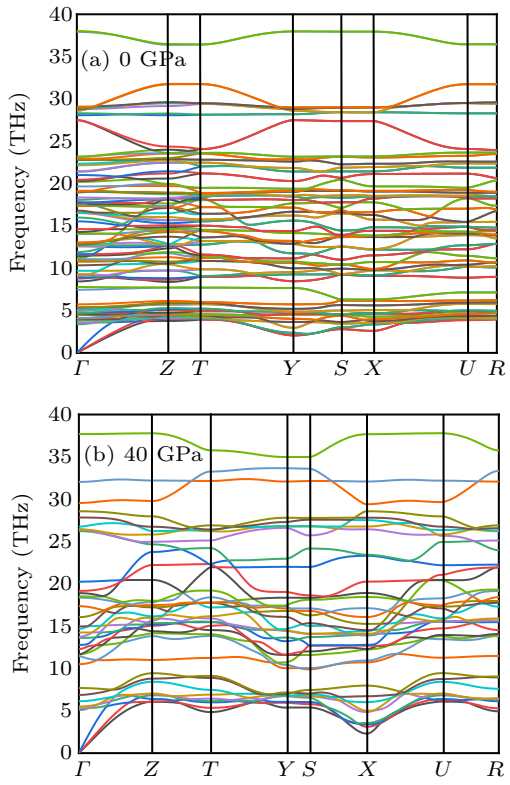



**Fig. 6.** The phonon-dispersion curves. (a) *Cmmm* phase at 0 GPa, and (b) *Pmmm* phase at 40 GPa, respectively.

To obtain a deep insight into the dynamical stabilities of the two considered structures, we calculated their phonon dispersion curves. As shown in Fig. 6(a), there are no imaginary phonon frequencies in the whole Brillouin zone for *Cmmm* structure indicates that it is dynamically stable at ambient conditions. From Fig. 6(b), there is no soft mode at any vectors in the whole Brillouin zone, suggesting the stability of *Pmmm* structure at 40 GPa. Besides, the vibrational bands of the optical part into higher frequencies at high pressure.

To further confirm the stabilization of the *Cmmm* structure, we studied its mechanical stabilities. Mechanical stability plays a crucial role in the stabilization of a crystal. The mechanical properties can also provide beneficial information for the stability and stiffness for materials. The elastic constants were obtained by fitting the stress of the strained structure and the strains. For an orthorhombic crystal, the elastic stability criteria are displayed as follows:

$$
\begin{aligned}
&C_{11}>0, C_{22}>0, C_{33}>0, C_{44}>0, C_{55}>0, C_{66}>0,\\
&[C_{11}+C_{22}+C_{33}+2(C_{12}+C_{13}+C_{23})]>0,\\
&(C_{11}+C_{22}-2C_{12})>0,\\
&(C_{11}+C_{33}-2C_{13})>0,\\
&(C_{22}+C_{33}-2C_{23})>0.
\end{aligned}
$$

All the elastic constants of the *Cmmm* structure and *Pmmm* structure were calculated in comparison with the other transition metal triborides $TMB_3$ ($TM$ = W, Cr, Os, and Ta) as seen in Table 1. As shown in Table 1, it is clear that the *Cmmm* structure satisfies these criteria, indicating that it is mechanically stable at zero pressure. So the *Cmmm* structure is both mechanically and dynamically stable at ambient conditions. The bulk modulus $B$ and shear modulus $G$ is calculated by using the elastic constants. Besides, Young's modulus $Y$ and Poisson's ratio $\upsilon$ are obtained by the equations $Y=(9BG)/(3B+G)$ and $\upsilon=(3B-2G)/(6B+2G)$. As seen in Table 1, the calculated $C_{22}$ for the *Cmmm* structure is bigger than $C_{11}$ and $C_{33}$, indicating that the resistance to deformation along the $b$ direction is stronger than that along $a$ and $c$ directions. Besides, the *Cmmm* structure has a $G$ value of 132 GPa, so it is supposed that this structure can endure the shearing strain to a great extend. Young's modulus can reflect the stiffness of materials. In Table 1, the Young's modulus of the six structures exhibit a sequence of $WB_3 > CrB_3 > OsB_3 > TaB_3 >$ *Cmmm* > *Pmmm*. As a result, a structure with a high $Y$ value has a greater stiffness than a structure with a low $Y$ value. Besides, the value of Poisson's ratio ($\upsilon$) can be used to describe the degree of directionality of the covalent bonding. From Table 1, we can be seen that all the $\upsilon$ value is below 0.33. Besides, the *Cmmm* structure has similar Poisson's ratio to that of $CrB_3$. The ratio value of $B/G$ is a criterion to describe the ductility or brittleness of materials. A $B/G$ value higher (or lower) than 1.75 is considered to be ductile (or brittle).[60] From Table 1, except $TaB_3$, the B/G values of the other phases are under the critical value, implying their brittle nature. The Vickers hardness is calculated by using the Chen's formula $H_v=2(K^2G)^{0.585}-3$, in which $G$ denotes the shear modulus and $K=G/B$, respectively. According to this formula, the hardness value of the *Cmmm* structure is calculated to be 23.8 GPa at ambient conditions. This suggests that the *Cmmm* structure is a potentially hard material.

**Table 1.** Calculated elastic constants (in unit GPa), bulk modulus $B$ (in unit GPa), shear modulus $G$ (in unit GPa), Young's modulus $Y$ (in unit GPa), Poisson's ratio $\upsilon$, and $B/G$ ratio of the *Cmmm* phase, *Pmmm* phase, $WB_3$, $CrB_3$, $OsB_3$, and $TaB_3$.

| Structure | | $C_{11}$ | $C_{22}$ | $C_{33}$ | $C_{44}$ | $C_{55}$ | $C_{66}$ | $C_{12}$ | $C_{13}$ | $C_{23}$ | $B$ | $G$ | $Y$ | $\upsilon$ | $B/G$ | $H_v$ |
|---|---|---|---|---|---|---|---|---|---|---|---|---|---|---|---|---|
| *Cmmm* | this work | 296 | 416 | 358 | 102 | 123 | 167 | 99 | 72 | 41 | 165 | 132 | 313 | 0.184 | 1.25 | 23.8 |
| *Pmmm* | this work | 278 | 468 | 268 | 123 | 144 | 151 | | | | 170 | 123 | 297 | 0.21 | 1.38 | 19.9 |
| $WB_3$ | theory[a] | 656 | | 479 | 277 | | | | | | 291 | 252 | 588 | 0.168 | 1.154 | 42 |
| $CrB_3$ | theory[b] | 623 | | 358 | 238 | | 246 | 131 | 141 | | 262 | 218 | 512 | 0.17 | 1.2 | 23.8 |
| $OsB_3$ | theory[c] | 525 | | 751 | 186 | | | 125 | 221 | | 317 | 195 | 482 | 0.245 | 1.63 | 36.9 |
| $TaB_3$ | theory[d] | 563 | 558 | 716 | 84 | 112 | 211 | 110 | 138 | 137 | 287 | 162 | 408 | 0.26 | 1.77 | 17.02 |

[a]Ref. [59], [b]Ref. [37], [c]Ref. [39], [d]Ref. [34].

To understand the bonding mechanism and origin of materials' physical properties, the electronic properties of the *Cmmm* and *Pmmm* phase were investigated by analyzing their total and partial density of states. From Fig. 7(a), we can see that the *Cmmm* phase exhibits metallic character, with the finite value of the DOS at the Fermi level. Y-4d and B-2p electrons occupy the major orbital, which is the leading cause for the metallicity. Moreover, there is no clear overlap of yttrium's d electron and boron's p electron in the range of −11 eV and 5 eV. From Fig. 7(b), we can also see that the *Pmmm* phase exhibits metallic character. Meanwhile, for the two phases, the Y-4d states and B-2p states contribute to most of DOS, and the B-2s states are mainly situated at the bottom of the valence bands.

To gain more in-depth insight into the bonding character of the predicted *Cmmm* structure, we calculated the electronic localization function (ELF). The electronic localization function (ELF) is widely used to describe chemical bonding. The ELF is a contour chart with the value from 0 to 1. Generally, ELF = 1 suggests the entire localization property, ELF = 0.5

offers homogeneous free-electron gas, and ELF = 0 suggests perfect delocalization. It is worthwhile to note that the bonding type of materials (metallic, covalent, and ionic bonding) can be determined based on the ELF. We plot the contours of ELF = 0.75 and (001) plane for the *Cmmm* structure. As shown in Fig. 8, there is the existence of a strong covalent B–B bonding in the *Cmmm* structure. Therefore, the strong covalent interaction between B–B bonds is the primary reason for its high hardness and stability.

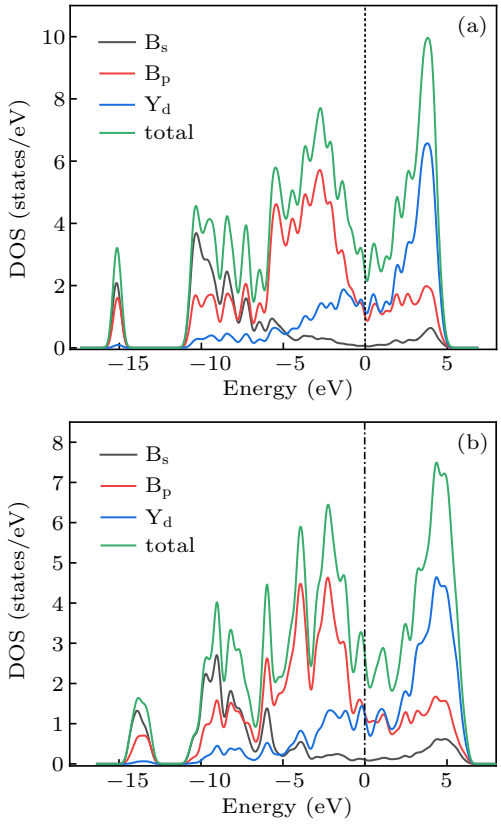



**Fig. 7.** Calculated total density of states (DOS) and partial density of states (PDOS) of the *Cmmm* phase (a), and *Pmmm* phase (b).

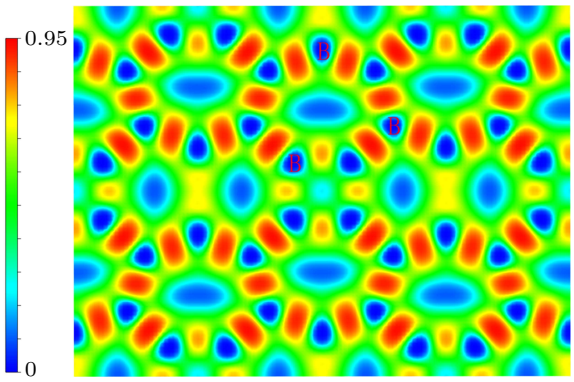



**Fig. 8.** The contours of the electronic localisation function (ELF) of the *Cmmm* phase on the (001) planes.

## 4. Conclusions

In summary, the calypso algorithm with first-principles calculations discovers two stable phases: one ground-state *Cmmm*-$YB_3$ and a high-pressure *Pmmm*-$YB_3$. These two phases are dynamically and elastically stable. The estimated Vickers hardness values are 23.8 GPa for the *Cmmm* phase at ambient conditions. This means that the *Cmmm* structure is a potentially low compressible and rigid material. Analysis of chemical bonding indicates that there are strong covalent and directional B–B bonds in *Cmmm*-$YB_3$. As we have updated the phase diagram of the Y–B system, we aim to stimulate a further experimental realization of boron-rich transition metal borides through our present theoretical investigation.

## References


[1] Haines J, Leger J and Bocquillon G 2001 *Ann. Rev. Mater. Res.* **31** 1
[2] Veprek S 2013 *J. Vac. Sci. Technol. A* **31** 050822
[3] Kaner R B, Gilman J J and Tolbert S H 2005 *Science* **308** 1268
[4] Brazhkin V V, Lyapin A G and Hemley R J 2002 *Philos. Mag. A* **82** 231
[5] Levine J B, Tolbert S H and Kaner R B 2010 *Adv. Funct. Mater.* **19** 3519
[6] Mounet N and Marzari N 2005 *Phys. Rev. B* **71** 205214
[7] Occelli F, Loubeyre P and LeToullec R 2003 *Nat. Mater.* **2** 151
[8] Zheng J C 2005 *Phys. Rev. B* **72** 052105
[9] Zhang Y, Sun H and Chen C F 2006 *Phys. Rev. B* **73** 144115
[10] Chung H Y, Weinberger M B, Levine J B, Kavner A, Yang J M, Tolbert S H and Kaner R B 2007 *Science* **316** 436
[11] Chung H Y, Weinberger M B, Yang J M, Tolbert S H and Kaner R B 2008 *Appl. Phys. Lett.* **92** 261904
[12] Cumberland R W, Weinberger M B, Gilman J J, Clark S M, Tolbert S H and Kaner R B 2005 *J. Am. Chem. Soc.* **127** 7264
[13] Gu Q F, Krauss G and Steurer W 2008 *Adv. Mater.* **20** 3620
[14] Li Q, Zhou D, Zheng W T, Ma Y M and Chen C F 2013 *Phys. Rev. Lett.* **110** 136403
[15] Lu C, Li Q, Ma Y M and Chen C F 2017 *Phys. Rev. Lett.* **119** 115503
[16] Tse J S, Klug D D, Uehara K and Li Z Q 2000 *Phys. Rev. B* **61** 10029
[17] Li Q, Zhou D, Zheng W T, Ma Y M and Chen C F 2015 *Phys. Rev. Lett.* **115** 185502
[18] Knappschneider A, Litterscheid C, Kurzman J, Seshadri R and Albert B 2011 *Inorg. Chem.* **50** 10540
[19] Niu H Y, Wang J Q, Chen X Q, Li D Z and Kolmogorov A N 2012 *Phys. Rev. B* **85** 144116
[20] Li B, Sun H and Chen C F 2014 *Phys. Rev. B* **90** 014106
[21] Gou H Y, Dubrovinskaia N, Bykova E, Tsirlin A A, Kasinathan D, Schnelle W, Richter A, Merlini M, Hanfland M, Abakumov A M, Batuk D, Tendeloo G V, Nakajima Y, Kolmogorov A N and Dubrovinsky L 2013 *Phys. Rev. Lett.* **111** 157002
[22] Zhang M G, Yan H Y, Zhang G T and Wang H 2012 *J. Phys. Chem. C* **116** 4293
[23] Xie M, Mohammadi R, Mao Z, Armentrout M M, Kavner A, Kaner R B and Tolbert S H 2012 *Phys. Rev. B* **85** 064118
[24] Mohammadi R, Xie M, Lech A T, Turner C L, Kavner A, Tolbert S H and Kaner R B 2012 *J. Am. Chem. Soc.* **134** 20660
[25] Wang S, Yu X, Zhang J, Zhang Y, Wang L, Leinenweber K, Xu H, Popov D, Park C, Yang W, He D and Zhao Y 2014 *J. Superhard Mater.* **36** 279
[26] Litterscheid C, Knappschneider A and Albert B 2012 *Z. Anorg. Allg. Chem.* **638** 1608
[27] Knappschneider A, Litterscheid C, George N C, Brgoch J, Wagner N, Beck J, Kurzman J A, Seshadri R and Albert B 2014 *Angew. Chem. Int. Ed.* **53** 1684
[28] Zhang M, Lu M C, Du Y H, Gao L L, Lu C and Liu H Y 2014 *J. Chem. Phys.* **140** 174505
[29] Gou H Y, Tsirlin A A, Bykova E, Abakumov A M, Van Tendeloo G, Richter A, Ovsyannikov S V, Kurnosov A V, Trots D M, Konôpková Z, Liermann H P, Dubrovinsky L and Dubrovinskaia N 2014 *Phys. Rev. B* **89** 064108
[30] Wu L, Wan B, Zhao Y, Zhang Y, Liu H, Wang Y, Zhang J and Gou H 2015 *J. Phys. Chem. C* **119** 21649
[31] Zhang G T, Gao R, Zhao Y R, Bai T T and Hu Y F 2017 *J. Alloys Compd.* **723** 802

[32] Zhang R F, Legut D, Lin Z J, Zhao Y S, Mao H K and Veprek S 2012 *Phys. Rev. Lett.* **108** 255502
[33] Zhang X Z, Zhao E J and Wu Z J 2015 *J. Alloys Compd.* **632** 37
[34] Wei S L, Li D, Lv Y Z, Liu Z and Cui T 2016 *Phys. Chem. Chem. Phys.* **18** 18074
[35] Zhang M G, Wang H, Wang H B, Cui T and Ma Y M 2010 *J. Phys. Chem. C* **114** 6722
[36] Yan Q, Wang Y X, Wang B, Yang J M and Yang G 2015 *RSC Adv.* **5** 25919
[37] Zhong M M, Kuang X Y, Wang Z H, Shao P, Ding L P and Huang X F 2013 *J. Chem. Phys.* **139** 234503
[38] Ying C, Bai X W, Du Y G, Zhao E J, Lin L and Hou Q Y 2016 *Int. J. Mod. Phys. B* **30** 1650131
[39] Ji Z W, Hu C H, Wang D H, Zhong Y, Yang J, Zhang W Q and Zhou H Y 2012 *Acta Mater.* **60** 4208
[40] Wang Y C, Yao T K, Wang L M, Yao J, Li H, Zhang J W and Gou H Y 2013 *Dalton Trans.* **42** 7041
[41] Huang L H, Zhao Y R, Zhang G T, Zhang M G, Li P Y and Hu Y F 2019 *Mol. Phys.* **117** 547
[42] Bai T T, Zhang G T, Zhao Y R, Chen L, Mu B X, Han Y F and Wei Q 2019 *Mol. Phys.* **118** e1603411
[43] Zhang X Y, Qin J Q, Sun X W, Xue Y N, Ma M Z and Liu R P 2013 *Phys. Chem. Chem. Phys.* **15** 20894
[44] Zhang G T, Bai T T, Zhao Y R and Hu Y F 2016 *Materials* **9** 703
[45] Jaeger B, Paluch S, Wolf W, Herzig P, Zogal O J, Shitsevalova N and Paderno Y 2005 *J. Alloys Compd.* **383** 232
[46] Waskowska A, Gerward L, Olsen J S, Babu K R, Vaitheeswaran G, Kanchana V, Svane A, Filipov V B, Levchenko G and Lyaschenko A 2011 *Acta Materialia* **59** 4886
[47] Wang Y C, Lv J, Zhu L and Ma Y M 2010 *Phys. Rev. B* **82** 094116
[48] Wang Y C, Lv J, Zhu L and Ma Y M 2012 *Comput. Phys. Commun.* **183** 2063
[49] Wang Y C, Lv J, Zhu L, Lu S, Yin K T, Li Q, Wang H, Zhang L J and Ma Y M 2015 *J. Phys.: Condens. Matter* **27** 203203
[50] Kresse G and Hafner J 1993 *Phys. Rev. B* **47** 558
[51] Kresse G and Hafner J 1994 *J. Phys.: Condens. Matter* **6** 8245
[52] Kresse G and J F 1996 *J. Phys. Rev. B* **54** 11169
[53] Perdew J P, Burke K and Ernzerhof M 1996 *Phys. Rev. Lett.* **77** 3865
[54] Kresse G and J F 1996 *Phys. Rev. B* **54** 11169
[55] Will G and Kiefer B 2001 *Z. Anorg. Allg. Chem.* **627** 2100
[56] Togo A, Oba F and Tanaka I 2008 *Phys. Rev. B* **78** 134106
[57] Togo A and Tanaka I 2015 *Scr. Mater.* **108** 1
[58] Chen X Q, Niu H Y, Li D Z and Li Y Y 2011 *Intermetallics* **19** 1275
[59] Liang Y C, Yuan X and Zhang W Q 2011 *Phys. Rev. B* **83** 220102
[60] Pugh S F 1954 *Philos. Mag.* **45** 823